Self-Repairable, High Permittivity Dielectric Elastomers with Large Actuation Strains at Low Electric Fields

*Simon J. Dünki, Yee Song Ko, Frank A. Nüesch, and Dorina M. Opris**

A one-step process for the synthesis of elastomers with high permittivity, excellent mechanical properties and increased electromechanical sensitivity is presented. It starts from a high molecular weight polymethylvinylsiloxane, P1, whose vinyl groups serve two functions: the introduction of polar nitrile moieties by reacting P1 with 3-mercaptopropionitrile (1) and the introduction of cross-links to fine tune mechanical properties by reacting P1 with 2,2′-(ethylenedioxy)diethanethiol (2). This twofold chemical modification furnished a material, C2, with a powerful combination of properties: permittivity of up to 10.1 at 10^4 Hz, elastic modulus $Y_{10\%} = 154$ kPa, and strain at break of 260%. Actuators made of C2 show lateral actuation strains of 20.5% at an electric field as low as 10.8 V μm^{-1}. Additionally, such actuators can self-repair after a breakdown, which is essential for an improved device lifetime and an attractive reliability. The actuators can be operated repeatedly and reversibly at voltages below the first breakdown. Due to the low actuation voltage and the large actuation strain applications of this material in commercial products might become reality.

1. Introduction

There is an increasing need for synthetic elastomers that respond to external stimuli and are easy to prepare and process.[1] Those elastomers that respond to an electric field by changing their size and shape are of great interest for many fields of applications.[2] Dielectric elastomer actuators (DEAs) are stretchable capacitors made of a thin elastic film coated with two compliant electrodes which expend their area when charged (**Figure 1**).[3] Due to their simple working principle and muscle-like actuation, DEA could find a large variety of applications in engines, optical devices, sensors, energy harvesters, and artificial muscles to name a few.[4] Since most elastomers do not contain electroactive components, the observed expansion is due to the electrostatic attraction forces of the unlike charges and repulsion forces of the like charges on the electrodes. One disadvantage of the DEA, which might hinder their applications, is a driving voltage in the kV regime. A key challenge in the DEA field is therefore to prepare an elastomer that actuates at a low voltage.

The actuation strain is given by

$$s = -\frac{p}{Y} = -\frac{\varepsilon'\varepsilon_0}{Y}E^2 \quad (1)$$

where s is the actuation, p is the electrostatic pressure, Y is the elastic modulus, ε' is the dielectric permittivity, $\varepsilon_0 = 8.854*10^{-12}$ F m^{-1} the vacuum permittivity, and E the electric field strength.[3] Thus, the driving voltage can be reduced by optimizing two material parameters: reducing Y and increasing ε'.[5] Elastomers with low Y can be prepared by reducing the cross-link density[6] or by adding a softener.[7] The reduction of Y increases the actuation strain but results in soft materials that have poor mechanical robustness and low output stress.

To increase the ε' of an elastomer two strategies are being pursued: blending with highly polarizable ceramic or conductive fillers and functionalization with polar groups.[8] The former can increase the permittivity of a material, but in most cases the mechanical properties are negatively affected. For some exceptions, see ref.[9] The latter includes functionalization of silicones with polar groups. When such material is subjected to an electric field, the randomly oriented dipoles will align with the field and the polymer chains will experience strain. This results in dimensional changes (Figure 1). Silicones have a siloxane (Si–O) backbone, which carries two organic hydrocarbon substituents per silicon. They have a low T_g which ensures elastic behavior well below room temperature. Therefore, by functionalizing silicones with pendant polar groups, it might be possible to prepare a material that shows increased permittivity while the T_g is still sufficiently low, despite of unavoidable increase in the T_g due to the dipole–dipole interactions. Silicones modified with polar trifluoropropyl, *p*-nitroaniline, nitrobenzene or cyanopropyl groups are known in the literature and they indeed show an increase in ε'.[10] However, the rather low molecular weight ($\bar{M}_w$) of these functionalized polymers did not allow formation of highly stretchable materials.

It was the aim of this work to synthesize an elastic material, which not only exhibits increased permittivity and good mechanical properties but at the same time, can also be

S. J. Dünki, Y. S. Ko, Prof. F. A. Nüesch, Dr. D. M. Opris
Swiss Federal Laboratories for Materials Science and Technology Empa
Laboratory for Functional Polymers
Ueberlandstr. 129, CH-8600 Dübendorf, Switzerland
E-mail: dorina.opris@empa.ch
S. J. Dünki, Y. S. Ko, Prof. F. A. Nüesch
Ecole Polytechnique Fédérale de Lausanne (EPFL)
Institut des matériaux
Station 12, CH-1015 Lausanne, Switzerland

DOI: 10.1002/adfm.201500077

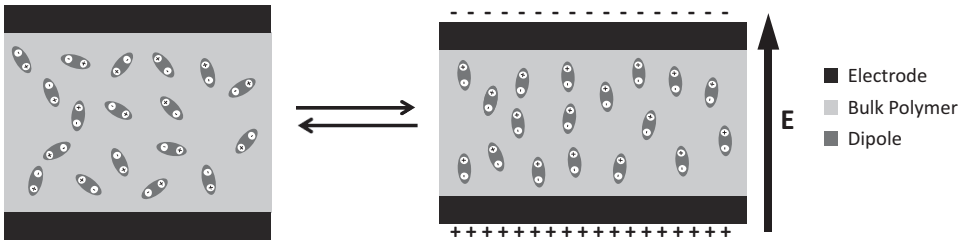

Figure 1. Working principle of a DEA that has as dielectric an elastomer carrying randomly attached polar groups (left) and the orientation of these groups in an electric field. The polymer chains experience strain and the film dimensions change (right).

actuated at low voltages. To achieve this, a high molecular weight polymethylvinylsiloxane **P1** was modified with polar nitrile groups to increase the permittivity while appropriate cross-linking allowed optimization of mechanical properties.

2. Results and Discussions

We focused on silicones because they promised creation of materials with still attractively low T_gs in spite of the T_g-increase unavoidably associated with the introduction of polar groups. To ensure good elastic properties and a high degree of polar group functionalization, a high $\bar{M}_w$ polymethylvinylsiloxane, **P1**, was used, which carries a vinyl group on every repeat unit. First, **P1** was synthesized by anionic ring opening polymerization of 1,3,5,7-tetravinyl-1,3,5,7-tetramethylcyclotetrasiloxane (V_4) in the presence of tetramethylammonium hydroxide (TMAH) (**Scheme 1**).[11] The molecular weight of **P1** and its distribution were determined as $\bar{M}_n$ = 59 kg mol^{-1}, $\bar{M}_w$ = 125 kg mol^{-1}, and D = 2.1 by GPC in tetrahydrofuran (THF) using polydimethylsiloxane standards. For the introduction of nitrile groups, 3-mercaptopropionitrile **1** was chosen, which was synthesized following standard procedures.[11]

Scheme 1 shows an overview of the attempts to synthesize materials functionalized with polar nitrile groups starting from **P1** and using different amounts of **1** (excess, less than equimolar, or at about equimolar amount of thiol **1** to the vinyl groups of **P1**) and different cross-linking reactions. When an excess of reagent **1** to polymer **P1** was used, nitrile functionalized polymer **P2** formed (Scheme 1a). Both the regiochemistry of the addition as well as its conversion were determined by ^{1}H NMR spectroscopy. The spectra in **Figure 2** show that the thiol addition proceeded predominantly in anti-Markovnikov fashion and that it was virtually quantitative. This latter point was concluded from the complete disappearance of the vinyl group proton signals between δ = 6.15 – 5.75 ppm and of the thiol group proton signal at δ = 1.77 ppm of the starting reagents, and the appearance of new signals in the aliphatic region (Figure 2).

Additionally, the FT-IR spectrum for the thiol-ene addition product shows no vibration band at 3054 and 1598 cm^{-1} characteristic for the C=C–H and C=C stretching. Our attempts to cross-link **P2** via a condensation reaction of the hydroxyl end-groups with

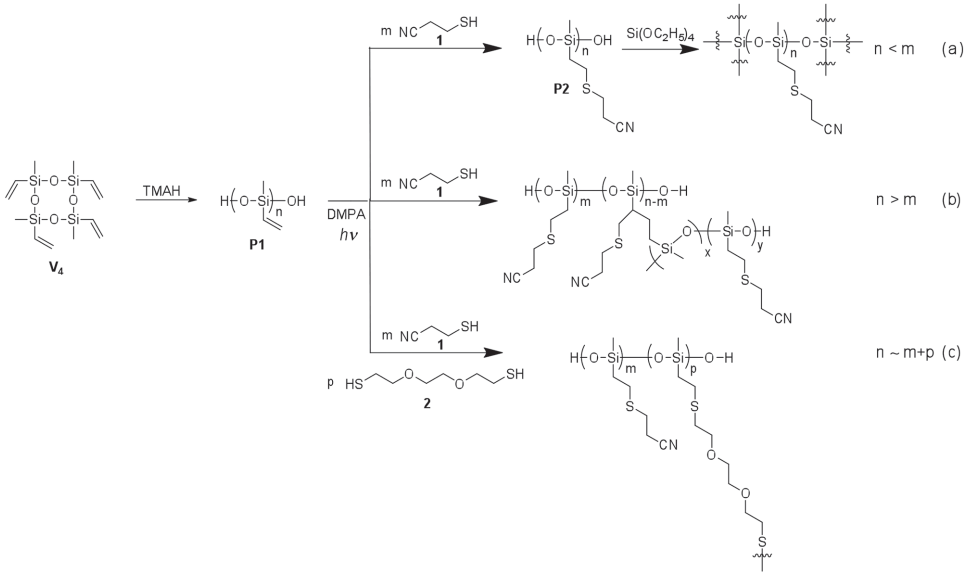

Scheme 1. Synthesis of polymethylvinylsiloxane **P1** from monomer V_4. The postpolymerization modification of **P1** with thiol **1** to polymer **P2**, which is cross-linked via a condensation with ETOS a) and in situ functionalization of **P1** with polar nitrile groups such that some vinyl groups are remaining which are used for cross-linking b) and c).

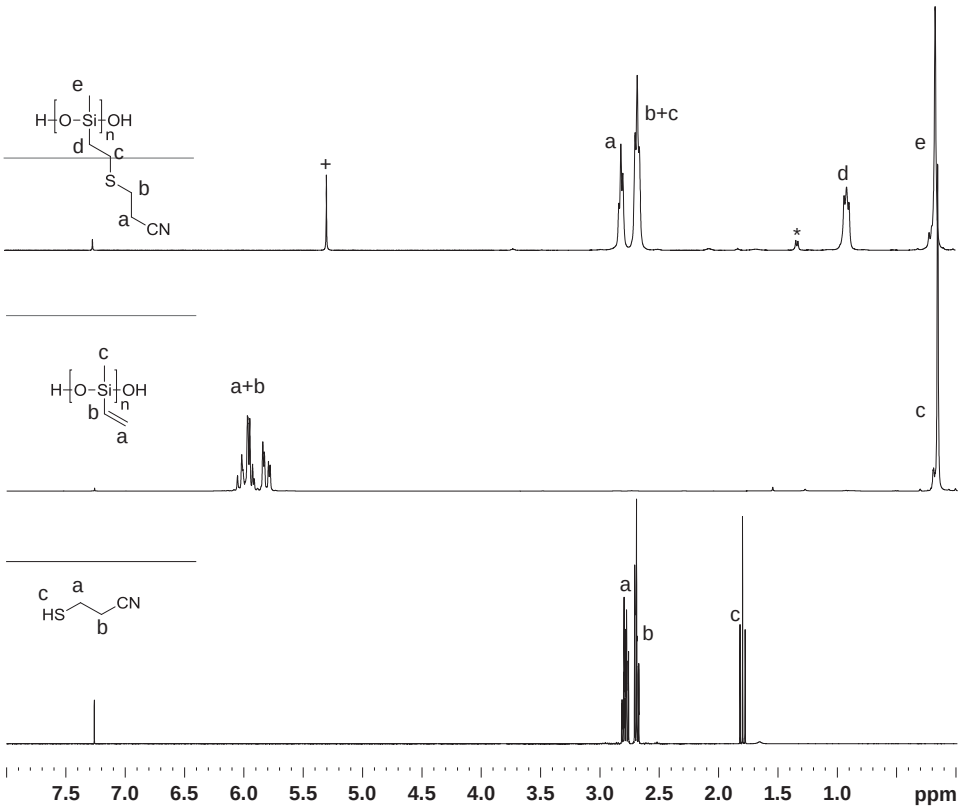

Figure 2. ^{1}H NMR spectra of polymethylvinylsiloxane **P1**, 3-mercaptopropionitrile **1**, and of the thiol-ene addition product **P2** in $CDCl_3$, dichloromethane (+), Markovnikov product (*).

ethyltetraethoxysilane (ETOS) in the presence of dibutyltin dilaurate catalyst were not successful (Scheme 1a). We however observed that when the stoichiometry between the thiol **1** and the vinyl groups in the thiol-ene addition was not respected, particularly when the vinyl groups were in excess, a cross-linked soft material with a low strain at break formed. Scheme 1b shows one of the possible reactions that affords cross-linking.[12] Although this may be considered disadvantageous, it offers a powerful opportunity to prepare thin films, whereby the dipole attachment and the cross-linking occur simultaneously. Thus, the UV irradiation of a thin film made of a solution of **P1**, less than equimolar amount of thiol **1** and 2,2-dimethoxy-2-phenylacetophenone (DMPA) allowed formation of a soft but brittle material. Our attempts to improve the mechanical properties of the film by using different amounts of thiol **1**, DMPA or surface functionalized silica were not successful (see Supporting Information). The highest strain at break for this kind of materials was only about 100%. Although disappointing, these experiments suggested, that it might be possible to prepare soft elastomers with improved elastic properties by further adjusting the cross-linking density. This was achieved by using 2,2′-(ethylenedioxy)diethanethiol (**2**) a bi-functional thiol as cross-linker (Scheme 1c). When a solution of **P1**, about equimolar amount of thiols (**1** and **2**) to the vinyl groups of **P1**, and DMPA was irradiated for few min with UV light, a soft material with good elastic properties formed. **Table 1** summarizes

Table 1. The characteristics of the starting polymers **P1** and the amount of reagents used for the synthesis of materials **A**, **B1**, **B2**, **B3**, **C1**, and **C2**.

Sample[a]	Starting polymer					**1** [mmol]	**2** [µl]	**2** [mmol]	Silica [%]
	Mw [kg mol^{-1}]	*Mn* [kg mol^{-1}]	PDI	m [g]	vinyl [mmol]				
A	125	59	2.1	2	23	21.8	20	0.12	–
B1	173	72	2.4	2	23	21.8	36	0.22	–
B2	173	72	2.4	2	23	21.8	32	0.20	–
B3	173	72	2.4	2	23	21.8	28	0.17	–
C1	173	72	2.4	2	23	21.8	34	0.21	2.5
C2	173	72	2.4	2	23	21.8	34	0.21	5

[a] For all samples, the amount of starting polymer (2 g), polar thiol (1.9 g), DMPA (25 mg), and toluene (2 mL) was kept constant.

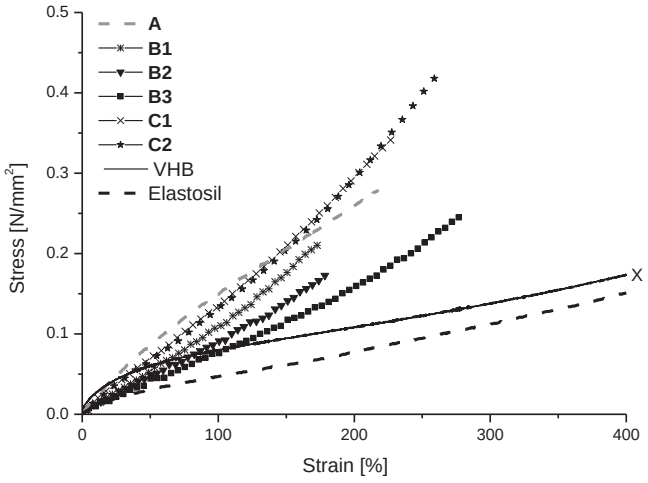

Figure 3. Stress–strain curves for materials **A**, **B1**-**B3** and **C1**, **C2** as well as of the VHB and Elastosil from standard tensile tests at 500 mm min^{-1}. The stress–strain curves were averaged from three independent tests. The strain at break for VHB and Elastosil was 850% and 770%, respectively.

the characteristics of the starting polymers **P1** and the amount of reagents used for the synthesis of different materials. For **P1** with $\bar{M}_w$ = 125 kDa, material **A** was obtained with a strain at break of 220% and $Y_{10\%}$ = 200 kPa (**Figure 3**).

To further optimize the elastic properties, a **P1** of higher molecular weight ($\bar{M}_n$ = 72 kg mol^{-1}, $\bar{M}_w$ = 173 kg mol^{-1}, and D = 2.4) was used for the synthesis of materials **B** and **C**. By decreasing the amount of dithiol **2**, a slight decrease in the elastic moduli at low strains from 110 to 90 and 80 kPa was observed for materials **B1**, **B2**, and **B3**, respectively (see **Table 2**). While the strain at break of materials **B1** and **B2** were quite similar, material **B3** prepared with less **2** had the highest strain at break of 280% (Figure 3) but viscoelastic losses were visually noted, e.g., after releasing the stress manually produced in this material, a slow recovery of the initial length of the sample was observed.

To reduce the viscoelastic losses, hexamethyldisilazane-treated silica particles were used (materials **C**). The concentration of silica was kept at low values to avoid stiffening (**C1** contains 2.5 wt% silica while **C2** contains 5 wt% silica). The stress–strain curves of **C1** and **C2** were almost superimposable, but an improvement in the strain at break for material **C2** (260%) was observed (Figure 3). The elastic moduli of **C** are higher than those of **B**, but still rather low (<150 kPa at all strains). Additionally, materials **C** were robust and not sticky and therefore easy to handle in thin films.

To verify the conversion of the vinyl groups in thin films, FT-IR spectra were recorded on pellets obtained by pressing the powder of ground **C2** film in KBr as well as on air and Teflon exposed surfaces of unground film (**Figure 4**). The change of the vibration band at 3055 cm^{-1} characteristic for the vinyl group was monitored in film after the reaction. The intensities of the vibration band of the vinyl groups for the Teflon-exposed surface and for the pellet are similar but much lower as compared with that of the vinyl groups by the air-exposed surface. The high concentration of vinyl groups observed for the air-exposed surface can be explained by the inhibition effect of oxygen. The appearance of a new vibration band at 2250 cm^{-1} characteristic for the nitrile group can be seen for the functionalized film. These results suggest that the thiol-ene addition functions well within the film, but is negatively affected for the air-exposed surface. Oxygen inhibition can be avoided by working under inert atmosphere. The incomplete conversion might be considered disadvantageous, but it offers a powerful tool for further functionalization. For example, the left-over vinyl groups can be used to interconnect layers in stacked actuators or to avoid delamination of electrodes in DEA devices.[13]

As is common, not all polymer chains were involved in network formation. The amount of uncross-linked material was determined by swelling/extraction tests (Table 2). The least amounts of noncross-linked material were observed for **A**, **C1**, and **C2** (<12%). The softest material **B3** disintegrated upon swelling and could therefore not be recovered properly.

Extension/relaxation tests were performed with **C2** (Supporting Information). The sample was strained from 0% to 100% strain at a rate of 20 mm min^{-1}. The stationary time at maximum strain was 2 min, while stationary time at minimum strain was 1 min. The excellent elastic properties of material **C2** are confirmed by the small hysteresis in this test. Additionally, dynamic mechanical analysis (DMA) has been carried out on a

Table 2. Elastic moduli at different strain levels as well as the elongation at break and the stress at break for the prepared materials. The percentage of extractable species (W_{ext}) obtained from swelling/extraction tests is also given.

Sample[a)]	$Y_{10\%}$ [kPa]	$Y_{20\%}$ [kPa]	$Y_{50\%}$ [kPa]	$Y_{100\%}$ [kPa]	Elong. [%]	Max. stress [N mm^{-2}]	W_{ext} [%]
A	200	180	140	120	220	0.28	11.3
B1	110	100	100	120	170	0.25	18.8
B2	90	100	90	90	180	0.18	21.1
B3	80	70	70	70	280	0.24	–
C1	160	130	130	140	230	0.35	10.3
C2	150	125	120	135	260	0.42	8.5
Elastosil	79	61	41	27	770	0.48	–
VHB	150	100	50	30	850	0.61	–

[a)]The elastic moduli were determined from the slope of the stress–strain curves using a linear fit to the data points within ±10% strain.

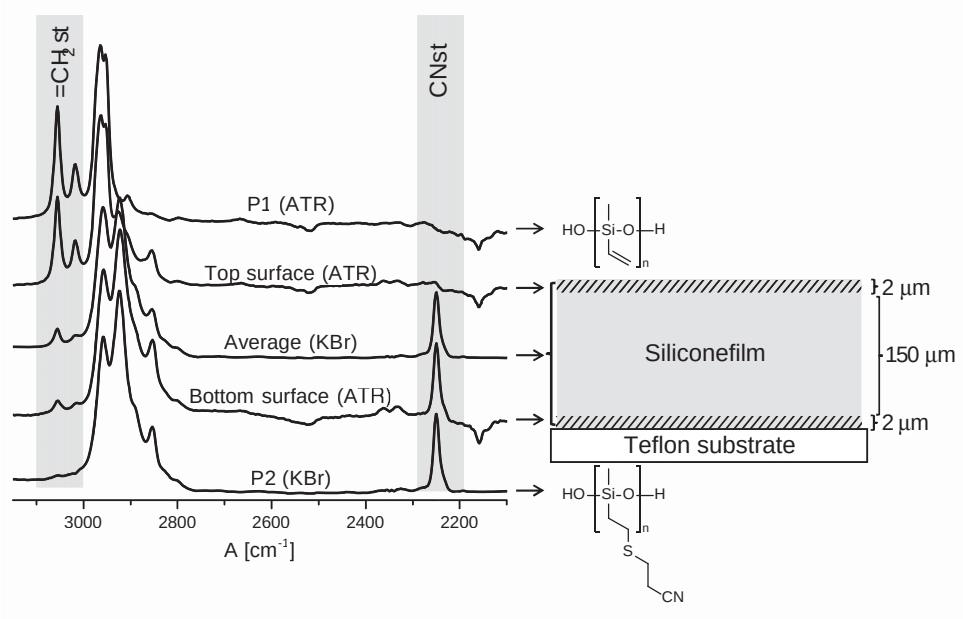

Figure 4. FT-IR spectra of the starting polymer **P1** (top), of polymer **P2** (bottom) and of the functionalized thin film recorded on different regions of the film (middle): on the air and Teflon exposed surface and on the ground film in KBr.

thin strip of **C2** (Supporting Information). A dynamic load of 2 g was applied to the sample at 1% strain and measurements were done in the frequency range of 0.01–10 Hz. Materials **A** and **C2** have almost constant values of the elastic moduli at different frequencies of less than 250 kPa and low viscoelastic losses (tan δ) of less than 0.1 at low frequencies.

To explore the temperature window where the described materials can be used, DSC and TGA analysis were performed. The DSC thermograms for materials **A**, **B**, and **C** exhibit a glass transition temperature at about –50 °C. [14] This T_g is much higher as compared with parent polymethylvinylsiloxane (T_g = –122 °C),[15] but still sufficiently low to allow the use of these materials at low temperatures. Additionally, these materials are also stable in air up to 250 °C (see Supporting Information). At this temperature, some residual volatiles are released. The maximum degradation occurred at about 395 °C and the amount of residue left is about 35%–40% (see Supporting Information).

Materials **A** and **C2** have the highest strain at break and lowest viscoelastic losses and were therefore selected for further investigations. Their mechanical, dielectric, and electromechanical properties were compared with that of commercial VHB 4905 foil and commercial Elastosil RT 745. The VHB foil is intensively used by the DEA community for the construction of devices.[16] The stress–strain curves show that the modified silicones are stiffer (e.g., for **A** $Y_{10\%}$ = 200 kPa and for **C2** $Y_{10\%}$ = 150 kPa) and have less strain at break (s_{max} = 260% for **C2**) as compared with VHB ($Y_{10\%}$ = 150 kPa) and Elastosil ($Y_{10\%}$ = 79 kPa) (Figure 3 and Table 2).

Figure 5 shows the dielectric properties as function of frequency at room temperature for materials **C2**, VHB foil, and Elastosil while **Table 3** summarizes the elastic moduli at 10% strain, the actuation strain at different voltages, the dielectric breakdown, as well as the permittivity at 10^4 Hz. This frequency was considered sufficiently high to eliminate the contribution of electrode polarization which is reflected by a large increase in the ε' at low frequencies. This increase is associated with an increase in the dielectric loss. The permittivity at high frequencies is ε' = 10.1 for **C2** and, thus, much higher than Elastosil (ε' = 3.0) and VHB foil (ε' = 4.5). A relaxation peak at about 500 Hz that results in an increase in the permittivity was observed for **C2**. The origin of this relaxation process is presently the subject of

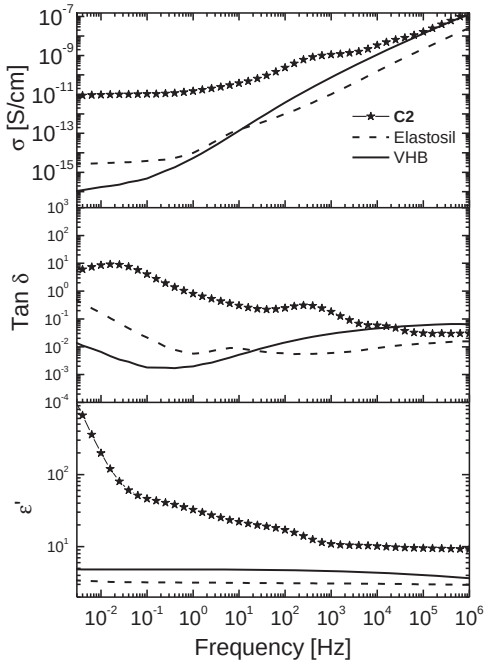

Figure 5. Permittivity (bottom), loss factor (middle), and conductivity (top) of material **C2**, Elastosil, and VHB foil as a function of frequency at room temperature.

Table 3. The permittivity (ε'), tan δ, conductivity (σ), $Y_{10\%}$, actuation strain at different electric fields (s_x), maximum actuation at breakdown, and the breakdown field (E_b) obtained from the actuators tests.

Sample	ε' at 10^4 Hz	Tan δ	σ [S cm^{-1}][a)]	$Y_{10\%}$ [kPa]	s_x [%] at 6 V μm^{-1}	s_x [%] at 8 V μm^{-1}	s_x [%] at 10 V μm^{-1}	s_x [%] at E_b	E_b [V μm^{-1}]
C2	10.1	0.059	9.5×10^{-12}	154	4.4	9.3	17.4	20.5	10.8
VHB	4.4	0.05	1.75×10^{-16}	152	0	0	0	–	>100
Elastosil	3	0.009	2.95×10^{-15}	79	0.2	0.4	0.7	6.0	25

[a)]The conductivity values were taken at 0.01 Hz, where the plateau was reached.

further investigations. The conductivity for the modified silicones decreases with decreasing frequency and is within the limits of dielectric materials ($\sigma = 9.5 \times 10^{-12}$ S cm^{-1}).

Materials **A** and **C2** were further evaluated in electromechanical tests. At least two independent actuator measurements were conducted for each material. It should be mentioned here that the circular actuators constructed from **A** and **C2** were 28.6% prestained while the actuators constructed from VHB foil were 300% prestrained (see Experimental Section). A stepwise increase in voltage (50 V every 2 s) was applied to the samples until breakdown through the material occurred. The determined actuation strains are shown in **Figure 6** as a function of the nominal electric field strength. The actuation strains at a certain voltage for **A** and **C2** were similar, but a significant improvement was observed for material **C2** with respect to the electrical breakdown and the maximum actuation strain. For example, the maximum actuation strain of **A** was 9.6% at 8.8 V μm^{-1}, while for **C2**, a maximum actuation strain of 20.5% at 10.8 V μm^{-1} was measured. High electric fields are required to actuate the VHB and Elastosil, while material **C2** is actuated at much lower electric fields. For a lateral actuation strain of 8% material **C2** required 7.4 V μm^{-1}, while Elastosil and VHB required higher electric fields of 24.0 and 64.2 V μm^{-1}, respectively. This represents a reduction of the electric field for **C2** by a factor of 8.5 and 3 as compared with VHB and Elastosil, respectively. Since **C2** is stiffer as compared with VHB and Elastosil, the increase in the actuation strain is due only to the increase in the ε' and not due to the increase of ε'/Y (see Equation ((1))). The maximum actuation strain of 20.5% at breakdown (10.8 V μm^{-1}) for **C2** was higher as compared with that of Elastosil (e.g., 8.6% at 24.6 V μm^{-1}). Material **C1** and Elastosil were also tested in actuators without prestrain (Figure 6 bottom). Also in these tests, the modified silicone has an actuation strain of 8% at 6.7 V μm^{-1}, while Elastosil shows a much lower actuation strain of 0.4% at the same electric filed. To the best of our knowledge, this is the highest lateral actuation strain at the lowest electric field reported to date for a silicone elastomer.

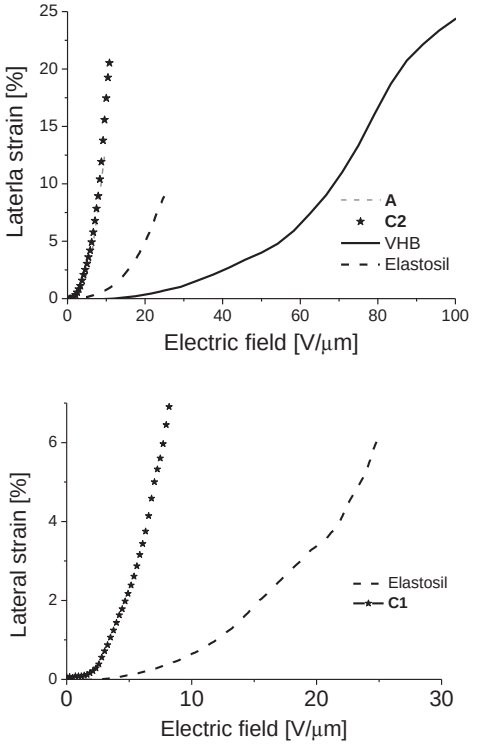

Figure 6. Lateral actuation strain membrane actuators for materials **A**, **C2** and Elastosil (each with 28.6% prestrain) as well as of VHB foil (300% prestrain) as a function of the applied voltage (top) and the lateral actuation strain of materials **C1** and Elastosil (both without prestrain) (bottom).

During the electromechanical tests, it was observed that the actuators constructed with **A** and **C2** were able to self-repair after a breakdown and resume actuation with the previous performance. Such effects have already been reported for actuators and were attributed either to the electrode material or to the dielectric used.[17–19] For example, Pei et al. showed that thin SWNT electrodes are able to self-clear due to localized degradation and loss of conductivity around the breakdown site.[17] A similar effect was observed by Opris et al. for a silicone/graphene composite electrode. It was shown that during a breakdown event, part of the electrode and dielectric film are burnt.[18] This burning process insulates the defect right, where the breakdown occurs. Furthermore, Anderson and co-workers also reported the self-healing of an actuator constructed from a silicone sponge saturated with silicone oil as dielectric.[19] The self-healing effect was attributed to the silicone oil, which flows into defects and thus re-establishes the dielectric structure. Since we used the same electrode material (carbon black powder) throughout and no such behavior was noted for Elastosil and VHB, we concluded that this process is due to the nature of the dielectric rather than the electrode. The self-repairing process is likely due to elimination of the conductive path caused by the sparks that form during the breakdown event. The spark may burn part of the electrode and the dielectric film, some of the dielectric is oxidized to silica and turns that part of actuator inactive. That this effect can be seen only for **C2** and not for regular PDMS might

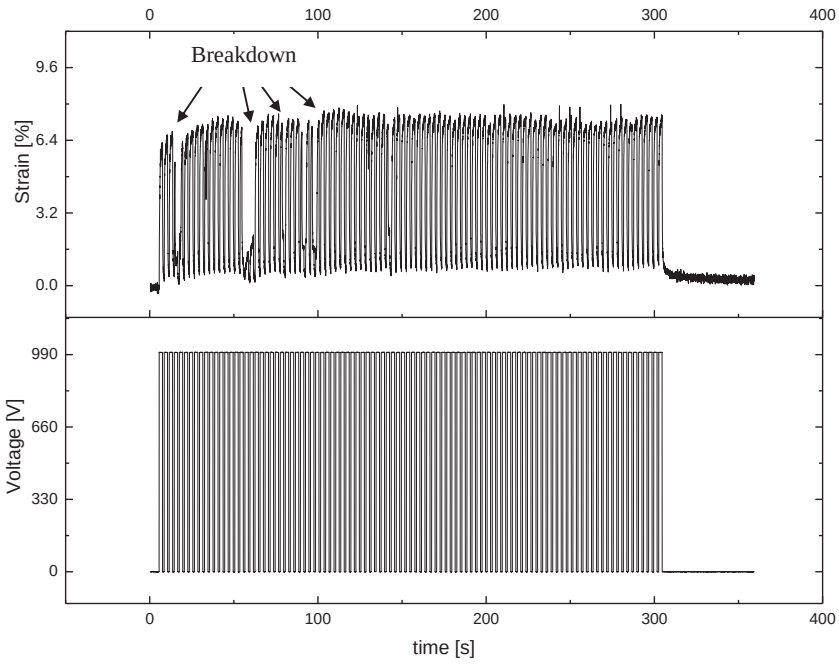

Figure 7. Long-term stability of an actuator made of **C2** membrane tested for 100 cycles at 0.33 Hz and electric field of 8.3 V μm^{-1}. Several breakdowns and self- repairing events can be seen.

be due to the high organic part of **C2** that can be burnt during the breakdown event. The dielectric is oxidized with formation of silica which insulates the defect. **Figure 7** shows a stability test with an actuator constructed from **C2** where 100 cycles near the breakdown field were performed. The breakdowns are marked with arrows. Already very shortly after each breakdown the performance is virtually back to normal.

The self-repair is observed both in alternating as well as in continuous voltage. **Figure 8** shows a **C2** membrane operated at a constant electric field of 5.5 V μm^{-1}. A fast actuation response is followed by several breakdowns and self-repairing events (left). When exactly the same actuator was tested at a slightly lower electric field of 5 V μm^{-1}, a constant actuation strain was observed (Figure 8 right). Such actuators can suffer several breakdowns and are nevertheless able to self-repair and function further. The actuators can be operated repeatedly and reversibly at voltages slightly below the first breakdown.

3. Conclusion

Here we report a one-step synthesis that allows formation of silicone elastomers with high permittivity, excellent mechanical properties, and increased electromechanical sensitivity. Given the simplicity of the synthesis process protocol, we expect our material to be scalable. The mechanical properties of these elastomers can be optimized via the amount of cross-linker, silica, and/or the molecular weight of the polymer used. The best material obtained has a permittivity of 10.1 at 10^4 Hz, an elastic modulus of 154 kPa at low strain, a strain at break of 260%, and a maximum lateral actuation strain of 20.5% at 10.8 V μm^{-1}. Additionally, the reliability of the DEAs constructed with this material is significantly improved due to their ability to self-repair after a breakdown.

4. Experimental Section

Materials and Characterization: Unless otherwise stated, all chemicals were reagent grade and used without purification. Tetramethylammonium hydroxide pentahydrate (TMAH) and 1,3,5,7-tetravinyl-1,3,5,7-tetramethylc yclotetrasiloxane (V_4) were purchased from ABCR. 2,2-Dimethoxy-2-pheny lacetophenone (DMPA), benzene, toluene, NaSH hydrate,

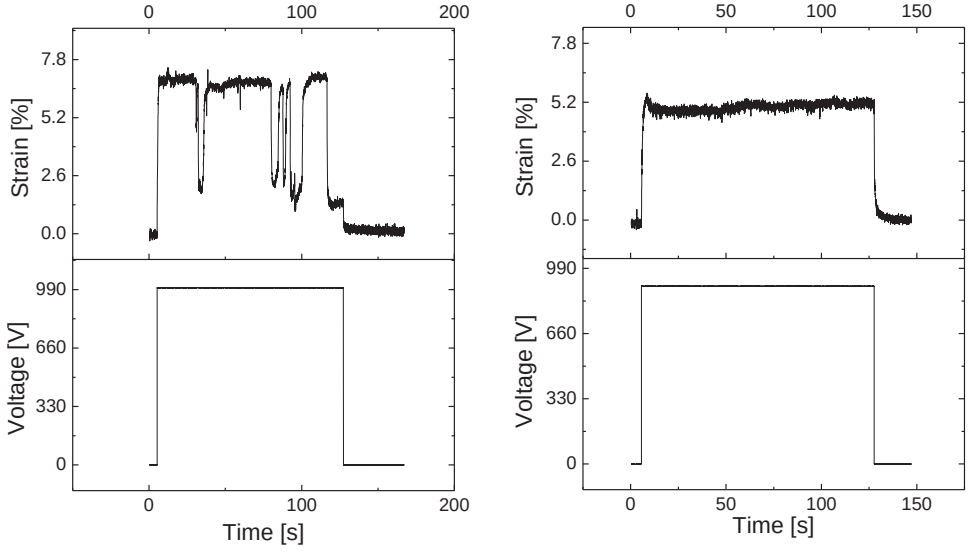

Figure 8. A 180 μm thick membrane actuator subjected to 1000 V for 120 s (left) and the same actuator subjected to 900 V for 120 s (right).

2,2′-(ethylenedioxy)diethanethiol, and acrylonitrile were purchased from Aldrich. Amorphous SiO_2 particles (60–70 nm) were purchased from US Research Nanomaterials Inc., Houston. Methanol, dichloromethane, hexane, ethyl acetate, and tetrahydrofurane were purchased from VWR and 1,1,1,3,3,3-hexamethyldisilazane from Alfa Aesar. Elastosil RT 745 "S" A + B (Wacker) was purchased from Drawin Vertriebs GmbH. VHB 4905 (3M) was kindly provided by Mr. M. Silvain (Empa). 3-Mercaptopropionitrile and **P1** were prepared according to the literature.[11] ^{1}H-, ^{13}C-, and ^{29}Si-NMR spectra were recorded at 298 K on a Bruker Avance 400 NMR spectrometer using a 5 mm broadband inverse probe at 400.13, 100.61, and 79.5 MHz, respectively. Chemical shifts (δ) in ppm are calibrated to residual solvent peaks ($CDCl_3$: δ = 7.26 and 77.16 ppm). Size exclusion chromatograms were taken with an Agilent 1100 Series HPLC (Columns: serial coupled PSS SDV 5 u, 100A and PSS SDV 5 u, 1000A, Detector: DAD, 235 nm and 360 nm; refractive index), THF was used as mobile phase. PDMS standards were used for the calibration and toluene as internal standard. Swelling extraction tests were conducted on materials **A**, **B,** and **C** which were extracted by immersion in toluene for 5 d, at room temperature. Every 24 h, the toluene was replaced. The films were then let dry in air and then in vacuum oven to constant mass. IR spectra were recorded on a Bruker Tensor 27 FT-IR with either an ATR setup or as KBr pellet in transmission. A mercury vapor UV-light source UVAHAND 250 GSH1 from Dr. Hönle AG without additional filters providing an irradiation intensity of 15 mW cm^{-2} in the frequency range between 320 and 600 nm was used. The tensile tests were performed using a Zwick Z010 tensile test machine with a crosshead speed of 500 mm min^{-1}. Tensile test specimens with a gauge width of 2 mm and a gauge length of 18 mm were prepared by die cutting. The strain was determined using a traverse moving sensor. The curves were averaged from three independent experiments. The tensile modulus was determined from the slope of the stress–strain curves using a linear fit to the data points within 10% strain. Dynamic mechanical analysis was carried out on a RSA 3 DMA from TA Instruments. Stripes 10-mm wide and 24-mm long were measured under a dynamic load of 2 g, at 1% strain in the frequency range of 0.01–10 Hz, at 26 °C, and 65% humidity. Permittivity measurements were done in the frequency range of 1 Hz to 1 MHz using an Novocontrol Alpha-A Frequency Analyzer. The V_{RMS} (root mean square voltage) of the probing AC electric signal applied to the samples was 1 V. Prior to the measurements, Au electrodes with a thickness of 30 nm were sputtered on both sides of the films. The permittivity was determined from the capacitance $C = \varepsilon\varepsilon_0 A/d$, where A is the electrode area, d is the thickness of the capacitor, and ε_0 is the vacuum permittivity. The electromechanical tests were performed using circular membrane actuators, for which the films were fixed between two circular frames. A biaxial prestrain of 28.6% was used. A higher prestrain was not tried since this might have caused mechanical damage. Circular electrodes (8 mm diameter) of carbon black powder were smeared on each side of the film with a fine brush. The connections to the electrodes were done using thin aluminum stripes. Photos of an actuator used for the electromechanical test and of the prestretching set-up are shown in the Supporting Information. A FUG HCL-35-12500 high voltage source served as power supply for actuator tests. The voltage was increased by 50 V every 2 s up to breakdown. The actuation strain was measured optically as the extension of the diameter of the electrode area via a digital camera, using an edge detection tool of a LabView program to detect the boundary between the black electrode area and the transparent silicone film.

*Methods (Synthesis of **P1**)*: Dry V_4 (70.70 g, 0.205 mmol) was added to dry TMAH (0.53 g, 0.24 mmol) in a schlenk flask and stirred for 1 h at RT, followed by additional 70 h stirring at 70 °C. The highly viscous polymer was then heated to 140 °C for 4 h. The unreacted cycles were then distilled in high vacuum at 140 °C for about 13 h. A highly viscous transparent polymer (66 g, 93%) was obtained. ^{1}H NMR ($CDCl_3$, 400 MHz): 6.07 – 5.88 (m, 2H, $=CH_2$); 5.84 – 5.74 (m, 1H, Si–CH=); 0.20 – 0.11 (m, 3H, Si–CH_3); GPC: $\bar{M}_n$ = 68 kg mol^{-1}, $\bar{M}_w$ = 171 kg mol^{-1}, D = 2.5. *Synthesis of **P2***: To **P1** (20.01 g, 232.2 mmol, 1 eq) dissolved in distilled THF (200 mL), **1** (40.48 g, 464.5 mmol, 2.0 eq) and DMPA (560 mg, 2.18 mmol, 0.009 eq) were added. The solution was then irradiated with a UV light for 20 min. The reaction mixture was concentrated under vacuum and precipitated in methanol (50 mL). The precipitation step was repeated several times. The product was dried in high vacuum at elevated temperatures to give yellowish highly viscous liquid. ^{1}H NMR (400 MHz, $CDCl_3$, δ): ^{1}H NMR ($CDCl_3$, δ): 2.85 – 2.78 (m, 2H, CH_2–CH_2–CN), 2.72 – 2.64 (m, 4H, CH_2–S–CH_2–CH_2–CN), 0.95 – 0.88 (m, 2H, Si–CH_2–), 0.18 (s, 3H, Si–CH_3); ^{13}C NMR ($CDCl_3$, δ): 118.8, 27.5, 26.6, 19.0, 18.1, 0.0; ^{29}Si NMR ($CDCl_3$, δ): 24.2; EA: Calcd.: C 41.58, H 6.40, N 8.08, S 18.5; found C 39.47, H 6.49, N 8.04, S 17.63.

General Synthesis of Polysiloxane Containing Ethylthiopropionitrile Elastomers: A solution of **P1**, **1**, **2**, surface functionalized silica particles and 2,2-dimethoxy-2-phenylacetophenone in toluene was casted to a film and initiated with UV light for few minutes. During this time, the dipole grafting to the silicone chains and the cross-linking occurred simultaneously. The films were dried at elevated temperature to constant mass before further testing were done. For the amount of reagents used please see Table 1.

Synthesis of Material C2: A solution of **P1** (2 g, 23 mmol vinyl groups), **1** (21.8 mmol), **2** (34 µL), surface functionalized silica particles (0.2 g dispersed in 4 mL toluene) and 2,2-dimethoxy-2-phenylacetophenone (11 mg, 0.04 mmol) in toluene (2 mL) was casted to a film using a doctor blade with 1200 µm gap and irradiated with a UV light for 2 min. During this time, the dipole grafting to the silicone chains and the cross-linking occurred simultaneously. The film was let drying at RT for 18 h and at 60 °C until constant mass.

Functionalization of SiO_2 Nanoparticles: 1,1,1,3,3,3-hexymethyldisilazan (9 g) was added to a dispersion of SiO_2 particles (15 g) in dry toluene (230 mL). The reaction mixture was stirred under argon for 18 h at RT. The dispersion was centrifuged, the supernatant discarded, and the remaining particles washed four times with toluene (4 × 100 mL). The particles were dried in HV for 48 h (14.8 g, 99%).

Thin Films of Elastosil: A mixture of Elastosil component A and B (1:1) was sonicated for 5 min in an ultrasonic bath to remove the air bubbles. Thin films were made by doctor blade technique on a teflon substrate and cured for 60 min at 100 °C.

Supporting Information

Supporting Information is available from the Wiley Online Library or from the author.

Acknowledgements

We gratefully acknowledge the financial support of Swiss National Science Foundation under the Swiss-Romanian Cooperation Program, Grant No. IZERZO_142215/1 (10/RO-CH/RSRP/01.01.2013), and the Swiss Federal Laboratories for Materials Science and Technology (Empa, Dübendorf). We gratefully acknowledge B. Fischer for DSC and TGA measurements, C. Walder and T. Künniger for DMA measurement, and Dr. G. Kovacs for providing us with the infrastructure for the actuator measurements (all Empa).

Received: January 7, 2015
Revised: February 11, 2015
Published online: March 16, 2015

[1] a) S. Ahn, R. M. Kasi, S. Kim, N. Sharma, Y. Zhou, *Soft. Mater* **2008**, *4*, 1151; b) M. Behl, A. Lendlein, *Soft Mater.* **2007**, *3*, 58.
[2] F. Carpi, D. De Rossi, R. Kornbluh, R. Perline, P. Sommer-Larsen, *Dielectric Elastomers as Electromechanical Transducers*, Elsevier, Amsterdam **2008**.
[3] R. Pelrine, R. Kornbluh, Q. Pei, J. Joseph, *Science* **2000**, *287*, 836.
[4] a) Y. Bar-Cohen, Q. Zhang, *MRS Bull.* **2008**, *33*, 173; b) F. Carpi, E. Smela, *Biomedical Applications of Electroactive Polymer Actuators*, Wiley-VCH, Weinheim, Germany **2009**.

[5] P. Brochu, Q. Pei, *Macromol. Rapid Commun.* **2010**, *31*, 10.
[6] M. Circu, Y. Ko, F. A. Nüesch, A. G. Christian, D. M. Opris, *Macromol. Mater. Eng.* **2014**, *299*, 1126.
[7] a) R. Shankar, T. K. Ghosh, R. J. Spontak, *Soft Matter* **2007**, *3*, 1116; b) X. Niu, H. Stoyanov, W. Hu, R. Leo, P. Brochu, Q. Pei, *J. Pol. Sci. B Pol. Phys.* **2013**, *51*, 197.
[8] a) G. Gallone, F. Carpi, D. De Rossi, G. Levita, A. Marchetti, *Mater. Sci. Eng. C* **2007**, *1*, 110; b) M. Molberg, D. Crespy, P. Rupper, F. Nüesch, J.-A. E. Manson, C. Löwe, D. M. Opris, *Adv. Funct. Mater.* **2010**, *20*, 3280; c) L. J. Romasanta, P. Leret, L. Casaban, M. Hernandez, M. A. de la Rubia, J. F. Fernandez, J. M. Kenny, M. A. Lopez-Manchado, R. Verdejo, *J. Mater. Chem.* **2012**, *22*, 24705; d) S. Risse S, B. Kussmaul, H. Krüger, G. Kofod, *Adv. Funct. Mater.* **2012**, *22*, 3958.
[9] a) F. Carpi, G. Gallone, F. Galantini, D. De Rossi, *Adv. Funct. Mater.* **2008**, *18*, 235; b) D. M. Opris, M. Molberg, C. Walder, Y. S. Ko, B. Fischer, F. A. Nüesch, *Adv. Funct. Mater.* **2011**, *21*, 3531; c) W. Hu, S. N. Zhang, X. Niu, C. Liu, Q. Pei, *J. Mater. Chem. C* **2014**, *2*, 1658.
[10] a) H. Böse, D. Uhl, R. Rabindranath, *Proc. SPIE* **2012**, *8340*: 83402E; b) S. Risse, B. Kussmaul, H. Krüger, G. Kofod, *Adv. Funct. Mater.* **2012**, *22*, 3958; c) B. Kussmaul, S. Risse, G. Kofod, R. Wache, M. Wegener, D. N. McCarthy, H. Krüger, R. Gerhard, *Adv. Funct. Mater.* **2011**, *21*, 4589; d) C. Racles, M. Cazacu, B. Fischer, D. M. Opris, *Smart Mater. Struct.* **2013**, *22*, 104004; e) C. Racles, M. Alexandru, A. Bele, V. E. Musteata, M. Cazacu, D. M. Opris, *RSC Adv.* **2014**, *4*, 37620; f) F. B. Madsen, L. Yu, A. E. Daugaard, S. Hvilsted, A. L. Skov, *Polymer* **2014**, *55*, 6212.
[11] a) G. P. Miller, A. P. Silverman, E. T. Kool, *Bioorg. Med. Chem.* **2008**, *16*, 56; b) D. W. Kang, B. C. Lee, *Polymer* **2004**, *28*, 143; c) M. Circu, Y. Ko, F. A. Nüesch, A. G. Christian, D. M. Opris, *Macromol. Mater. Eng.* **2014**, *299*, 1126.
[12] A. B. Löwe, *Polym. Chem.* **2010**, *1*, 17.
[13] G. Kovacs, L. Düring, S. Michel, G. Terrasi, *Sens. Actuators A* **2009**, *155*, 299.
[14] C. Racles, M. Alexandru, A. Bele, V. E. Musteata, M. Cazacu, D. M. Opris, *RSC Adv.* **2014**, *4*, 37620.
[15] S. J. Clarson, J. A. Semlyen, *Siloxane Polymers*, Prentice-Hall, Englewood Cliffs, NJ **1993**.
[16] I. A. Anderson, T. A. Gisby, T. G. McKay, B. M. O'Brien, E. P. Calius, *J. Apl. Phys.* **2012**, *112*, 041101
[17] a) H. Stoyanov, P. Brochu, X. Niu, C. Lai, S. Yun, Q. Pei, *RSC Adv.* **2013**, *3*, 2272; b) W. Yuan, H. Li, P. Brochu, X. Niu, Q. Pei, *Intern. J. Smart Nano Mater.* **2010**, *1*, 40; c) W. Yuan, L. Hu, Z. Yu, T. Lam, J. Biggs, S. M. Ha, D. Xi, B. Chen, M. K. Senesky, G. Grüner, Q. Pei, *Adv. Mater.* **2008**, *20*, 621.
[18] S. Michel, B. T. T. Chu, S. Grimm, F. A. Nüesch, A. Borgschulte, D. M. Opris, *J. Mater. Chem.* **2012**, *22*, 20736.
[19] S. Hunt, T. G. McKay, I. A. Anderson, *Appl. Phys. Lett.* **2014**, *104*, 113701.